Atmos. Chem. Phys. Discuss., doi:10.5194/acp-2016-772, 2016
Manuscript under review for journal Atmos. Chem. Phys.
Published: 31 August 2016

Effects of Cloud Condensation Nuclei and Ice Nucleating Particles on Precipitation Processes and Supercooled Liquid in Mixed-phase Orographic Clouds

Jiwen Fan[1*], L. Ruby Leung[1], Daniel Rosenfeld[2], Paul J. DeMott[3]

[1] Atmospheric Science & Global Change Division, Pacific Northwest National Laboratory, Richland, WA 99352

[2] Institute of Earth Sciences, The Hebrew University of Jerusalem, Jerusalem, 91904 Israel

[3] Department of Atmospheric Science, Colorado State University, Fort Collins, Co, 80523

- Corresponding author:

  jiwen.fan@pnnl.gov

Atmos. Chem. Phys. Discuss., doi:10.5194/acp-2016-772, 2016
Manuscript under review for journal Atmos. Chem. Phys.
Published: 31 August 2016

Atmospheric Chemistry and Physics Discussions

Abstract

How orographic mixed-phase clouds respond to the change of cloud condensation nuclei (CCN) and ice nucleating particles (INPs) are highly uncertain. The main snow production mechanism in warm and cold mixed-phase orographic clouds (referred to as WMOC and CMOC, respectively, distinguished here as those having cloud tops warmer and colder than -20°C) could be very different. We quantify the CCN and INP impacts on supercooled water content, cloud phases and precipitation for a WMOC and a CMOC case with a set of sensitivity tests. It is found that deposition plays a more important role than riming for forming snow in the CMOC, while the role of riming is dominant in the WMOC case. As expected, adding CCN suppresses precipitation especially in WMOC and low INP. However, this reverses strongly for CCN > 1000 cm^{-3}. We find a new mechanism through which CCN can invigorate mixed-phase clouds over the Sierra Nevada Mountains and drastically intensify snow precipitation when CCN concentrations are high (1000 cm^{-3} or higher). In this situation, more widespread shallow clouds with greater amount of cloud water form in the valley and foothills, which changes the local circulation through more latent heat release that transports more moisture to the windward slope, leading to much more invigorated mixed-phase clouds over the mountains that produce higher amounts of snow precipitation. Increasing INPs leads to decreased riming and mixed-phase fraction in the CMOC but has the opposite effects in the WMOC, as a result of liquid-limited and ice-limited conditions, respectively. However, it increases precipitation in both cases due to an increase of deposition for the CMOC but enhanced riming and deposition in the WMOC. Increasing INPs dramatically reduces supercooled water content and increases the cloud glaciation temperature, while increasing CCN has the opposite effects with much smaller significance.

Atmos. Chem. Phys. Discuss., doi:10.5194/acp-2016-772, 2016
Manuscript under review for journal Atmos. Chem. Phys.
Published: 31 August 2016

1. Introduction

Snowpack in the Sierra Nevada Mountains is California's largest source of fresh water. Understanding the factors contributing to snow precipitation over the mountains has important implications to predicting the hydrology and local climate of the western U.S. This has motivated a series of CalWater field campaigns carried out since 2009 to improve understanding of processes influencing precipitation and water supply in California. Supercooled liquid occurred commonly in clouds over the Sierra Nevada during the cold season (Rosenfeld et al., 2013). Closely linked to precipitation is the distribution of cloud liquid and ice phases, which may be influenced by supercooled liquid commonly occurring in orographic clouds (Rosenfeld et al., 2013). Besides precipitation, cloud radiative forcing and cloud feedback in the climate system are also highly dependent on cloud phases because of the very different radiative effect of liquid and ice particles. Hence understanding the key processes and factors impacting cloud phases is critical, but our lack of understanding and ability to model supercooled liquid and cloud phases is limiting skillful predictions at weather and climate time scales.

Many factors such as large-scale dynamics, solar heating, and aerosol particles can impact cloud properties and precipitation over the Sierra Nevada Mountains (Shen et al., 2010; Rosenfeld et al., 2008). Atmospheric rivers (ARs) are one of the primary large-scale dynamical features that bring large amount of water vapor from tropics to the U.S. west coast, and can create extreme rainfall and floods (Bao et al 2006; Ralph et al. 2011; Neiman et al. 2010). Aerosols in the atmosphere can modify cloud microphysical processes and potentially alter the location, intensity, and type of precipitation (Tao et al., 2012) by acting as cloud condensation nuclei (CCN) or ice nucleating particles (INPs). In California, pollution aerosols from the densely populated coastal plains and the Central Valley may be incorporated into the frontal airmass before orographic ascent and influence precipitation in the Sierra Nevada Mountains

Atmos. Chem. Phys. Discuss., doi:10.5194/acp-2016-772, 2016
Manuscript under review for journal Atmos. Chem. Phys.
Published: 31 August 2016

(Rosenfeld and Givati, 2006). Long-range transported aerosols (mainly dust particles) have also been found to have a potential influence on clouds and precipitation in the winter and spring seasons (Uno et al., 2009; Ault et al., 2011; Creamean et al., 2013).

Aerosol impacts can strongly depend on aerosol properties, but also dynamics, and thermodynamics. Many studies have shown that CCN can reduce warm rain precipitation from orographic clouds by reducing the efficiency of cloud droplets conversion into raindrops (e.g., Lynn et al., 2007; Rosenfeld and Givati, 2006; Jirak and Cotton, 2006) and can reduce snowfall precipitation due to reduced riming efficiency (Lowenthal et al., 2011; Rosenfeld et al., 2008). However, some recent studies show a possibility of increased precipitation by CCN in orographic mixed-phase clouds (Fan et al., 2014; Xiao et al., 2015). Other studies have shown that CCN may not have significant effect on the total precipitation, but rather shift precipitation from the windward to leeward slope; a so-called "spillover effect" (Saleeby et al., 2011; 2013). By acting as INPs, aerosols can enhance ice growth processes such as deposition and riming and thereby significantly increase snow precipitation (Fan et al., 2014). Both observational and modeling studies have shown that long-range transported dust particles can enhance orographic precipitation in California by serving as INPs (Ault et al., 2011; Creamean et al., 2013; Fan et al., 2014).

Besides precipitation, aerosols may have significant impacts on cloud phase and supercooled water content (SCW) in the mixed-phase clouds, which directly change cloud radiative forcing and Earth's energy balance. Modeling studies have shown that CCN tend to increase SCW via the processes such as suppressed warm rain and/or reduced riming efficiency (Khain et al., 2009; Ilotoviz et al., 2016; Saleeby et al., 2013). A recent observational study corroborated that increasing CCN decreases the cloud glaciation temperature and thus increases

Atmos. Chem. Phys. Discuss., doi:10.5194/acp-2016-772, 2016
Manuscript under review for journal Atmos. Chem. Phys.
Published: 31 August 2016

Atmospheric Chemistry and Physics
Open Access
Discussions

the abundance of the mixed-phase regime (Zipori et al., 2015). With abundant INPs such as dust particles, cloud glaciates at a much warmer temperature (Rosenfeld et al., 2011; Zipori et al., 2015). It is found that commonly occurring supercooled water in the clouds near the coastal regions of the western U.S. is associated with low CCN and limited INP conditions (Rosenfeld et al., 2013).

Recent evaluation of the Community Atmosphere Model version 5 (CAM5) with the Cloud-Aerosol Lidar and Infrared Pathfinder Satellite Observation (CALIPSO) satellite data showed that the model has insufficient liquid cloud and excessive ice cloud from the mid-latitudes to the polar regions, and liquid deficit bias maximizes over the Southern Ocean where supercooled water is prevalent (Kay et al., 2016). For cloud model simulations with cloud-resolving models, ice nucleation parameterizations often need to be modified in order to produce the mixed-phase clouds in the Arctic region (Fan et al., 2009; Fridlind et al., 2007). Considering many microphysical processes are sensitive to aerosol types (CCN or INP), temperature, and/or supersaturation (e.g., deposition growth), aerosol impacts on cloud phase can be complicated, depending on cloud dynamics and thermodynamics. Our current understanding of cloud microphysical processes impacting SCW and cloud phase in different meteorological environments is poor. Therefore, it is important to conduct process-level studies to improve our understanding.

Fan et al. (2014) conducted a study for two mixed-phase orographic cloud cases with different cloud temperatures and showed different significance of the CCN and INP impacts between the two cases. The two cases are February 15-16, 2011 (FEB16), and Mar 1-2, 2011 (MAR02). FEB16 has a cloud top temperature as cold as -32°C while the cloud top temperature of MAR02 is generally warmer than -20°C. The temperature differences at the same altitude

Atmos. Chem. Phys. Discuss., doi:10.5194/acp-2016-772, 2016
Manuscript under review for journal Atmos. Chem. Phys.
Published: 31 August 2016

between the two cases are about 6-10°C. For these reasons, we will herein refer to them as cold mixed-phase orographic clouds (CMOC) and warm mixed-phase orographic clouds (WMOC), respectively. The main snow-forming mechanism in warm and cold mixed-phase orographic clouds could be very different and lead to different precipitation response to changes of CCN and INP. Following Fan et al. (2014) this study aims to (1) understand the dominant ice growth processes in these two mixed-phase cloud systems; (2) quantify the response of precipitation to the changes of CCN and INP over a wide range from extremely low to extremely high concentrations, and (3) examine CCN and INP impacts on SCW and cloud phases. The same WRF model with the spectral-bin microphysics (SBM) as used in Fan et al. (2014) is employed. Ice nucleation is parameterized in dependence on mineral dust/biological particle concentrations on the basis of observational evidence. To better realize our science goals, the simulation resolution is further increased to be 1-km and the simulations are driven with the 2-km resolution baseline simulation from Fan et al. (2014).

2. Model Description and Simulation Design

2.1 Model description

As in Fan et al. (2014), simulations are performed using WRF version 3.1.1 developed at the National Center for Atmospheric Research (NCAR) (Skamarock et al., 2008) coupled with a spectral-bin microphysics (SBM) model (Khain et al., 2009; Fan et al., 2012). The SBM is a fast version of the full SBM described by Khain et al. (2004), in which ice crystal and snow (aggregates) in the full SBM are calculated based on one size distribution with separation at 150 μm. ice crystal and snow are referred to as low-density ice. Graupel and hail in the full SBM are grouped as high-density ice, represented with one size distribution without separation. More details about SBM that we used in this study can be found in Fan et al. (2014).

As discussed in Fan et al. (2014), hereafter referred to as FAN2014, the ice nucleation parameterizations in the SBM used for this study have been modified. A new ice nucleation parameterization of DeMott et al. (2015; cited as DeMott et al., 2013 in FAN2014 before the parameterization was published) was incorporated to SBM to investigate the impacts of dust as INPs. The parameterization connects nucleated ice particle concentration under a certain atmospheric condition with aerosol particle number concentration with diameter larger than 0.5 μm ($n_{a>0.5\mu m}$ in Eq. 2 of DeMott et al., 2015), which is referred to as INP concentration. In FAN2014, the aerosol particles that are connected with the DeMott et al. (2015) parameterization are referred to as "dust/bio" (from single particle mass spectral composition measurements), and are based on observations from the Passive Cavity Aerosol Spectrometer Probe (PCASP) for particles with diameter larger than 0.5 μm from clear-sky aircraft data. Note that the actual INP number concentration in the DeMott et al. (2015) parameterization includes an exponential temperature dependence that acts on aerosol concentration, and that the exponent on aerosol concentration is 1.25, but for simplicity in this paper we refer to the constant $n_{a>0.5\mu m}$ as the INP concentration. It should also be noted that the parameterization is designed and implemented as immersion freezing, that is, a pre-existing liquid particle (droplet or drop) is consumed for each formed ice crystal determined by the parameterization (at the same time, an ice nucleus is removed from the INP category). An added feature of implementation was to assume that the largest drops freeze first, followed by the smaller ones over the size spectrum of water drops when ice nucleation occurs. This implementation yielded the majority of observed large ice particles, as discussed in FAN2014. This assumption also acknowledges the expectation that the largest droplets should have a higher probability of containing an INP active at a given temperature. For contact freezing, we adopt the implementation of Muhlbauer and Lohmann (2009) for the parameterizations described in Cotton et al. (1986) and Young (1974) to connect with INP. The contribution from the contact freezing with this parameterization is negligible. As described in FAN2014, INP is a prognostic variable and over-nucleation is prevented by applying an upper limit of ice particle concentration.

2.2 Design of numerical experiments

In FAN2014, simulations were done for the two nested domains with a horizontal grid-spacing of 10 and 2 km, respectively. To focus on the orographic clouds over the Sierra Nevada Mountains and provide a better process-level understanding, we conduct new simulations using a smaller domain of 300 km × 280 km with a grid-spacing of 1 km (the yellow box in Fig. 1a) nested within the 2-km grid-spacing domain of FAN2014 (the blue box). The domain grid points are 301×281 horizontally with 51 vertical levels. The initial and lateral boundary conditions are produced from the baseline simulations of the 2-km grid-spacing in FAN2014 that were validated by various observational data. The lateral boundary data are updated every 3-hours. The RRTMG shortwave and longwave radiation schemes are used to account for aerosol-cloud-radiation interactions based on the droplet effective radius calculated by SBM.

CCN in the model is represented by a spectrum with 33 size bins with prognostic CCN number concentration for each bin. As stated above, the INP denotes the dust/bio particle number concentration in this region. For the purpose of this study, we conduct sensitivity tests by varying CCN and INP (i.e., dust/bio particle) concentrations over a wide range from the extremely low to extremely high concentrations as shown in Table 1. The initial CCN concentrations for the sensitivity simulations are set to be 30, 100, 300, 1000, and 3000 cm^{-3} (referred to as CCN30,

Atmos. Chem. Phys. Discuss., doi:10.5194/acp-2016-772, 2016
Manuscript under review for journal Atmos. Chem. Phys.
Published: 31 August 2016

CCN100, CCN300, CCN1000, and CCN3000 respectively). For each CCN condition, simulations are conducted with the initial INP concentration of 0.1, 1, 10, and 100 cm^{-3}, respectively, referred to as IN0.1, IN1, IN10, and IN100. Note that 100 cm^{-3} dust/bio means ~100 L^{-1} actual nucleated ice particles at -20^{o}C and 1000 L^{-1} at -25^{o}C using DeMott et al. (2015). The vertical profiles of CCN and INP number concentrations at the initial time are uniform below 6 km since observations do not show significant vertical variations as discussed in FAN2014. Simulations are conducted for both cases, and start at 12:00 pm UTC and run for 12 hours since the majority of the convective orographic clouds occur during this period. Note the observed CCN (INP) concentrations for CMOC and WMOC are around 30 (2) and 120 (4) cm^{-3}, respectively.

The CMOC case on FEB16 has cloud top temperatures about 10 degrees colder than the WMOC case on MAR02, and has higher relative humidity (RH) due to the lower temperature although the water vapor mixing ratio is much smaller (Fig. 1b-1d). Both cases are under the influence of atmospheric rivers that provide ample water vapor supply. We note however that the lower-level wind directions in the two cases are different, with prevailing westerly and northwesterly on FEB06, and southerly and southwesterly on MAR02.

3. Results

3.1 CMOC – FEB16

3.1.1 Precipitation and microphysical processes

Fig. 2a shows the accumulated surface precipitation averaged over the domain for the CMOC case (FEB16). Increasing INPs generally enhances the domain-averaged precipitation except at extremely high CCN concentration (i.e., 3000 cm^{-3}), as a result of increased snow

Atmos. Chem. Phys. Discuss., doi:10.5194/acp-2016-772, 2016
Manuscript under review for journal Atmos. Chem. Phys.
Published: 31 August 2016

precipitation (Fig. 2c). The sensitivity to INP concentration gets much smaller when INPs are 10 cm^{-3} and larger. Under the low INP condition where the liquid regime is dominant, the precipitation is first suppressed as CCN increase up to a polluted condition of 1000 cm^{-3} (grey arrow). This behavior is similar to the CCN effects on shallow warm clouds. As INP is further increased and mixed-phase clouds are increased, the decreased trend of precipitation with the increase of CCN is changed to a monotonic increasing trend as shown by the brown arrow in Fig. 2a. The most significant feature of Fig. 2a is the sharp increase of surface precipitation from CCN of 1000 to 3000 cm^{-3}, even at the extremely low INP condition. This is inconsistent with our previous understanding for deep mixed-phase clouds that precipitation should be significantly suppressed under the extremely polluted conditions because droplets get too small to growth efficiently and the riming also becomes very inefficient (Fan et al., 2007; Li et al., 2008). From Figs. 2b and 2c showing the liquid and snow mass concentrations near the surface (i.e., at the lowest model level of ~ 40 m above the ground), respectively, we see that (1) snow dominates the precipitation for the CMOC case and the ratio of warm rain to total precipitation is very small; and (2) the dramatically enhanced snow explains the sharp increase of precipitation from CCN of 1000 to 3000 cm^{-3}. Note that increasing CCN enhances snow precipitation under any INP condition (Fig. 2c), and warm rain is totally shut off when CCN are 1000 cm^{-3} or larger at INP of 0.1 cm^{-3} (Fig. 2b) due to the much smaller sizes of droplets.

By looking at the in-cloud microphysical properties as shown in Fig. 3, increasing CCN enhances snow number concentration and mass mixing ratio (N_s and Q_s, respectively). Especially, we see a large increase of snow mass from CCN1000 to CCN3000. Cloud ice number concentration and mass mixing ratio (N_i and Q_i, respectively) is also increased. Note ice and snow are represented with a single size spectrum and a threshold size of 150 μm in radius is used

Atmos. Chem. Phys. Discuss., doi:10.5194/acp-2016-772, 2016
Manuscript under review for journal Atmos. Chem. Phys.
Published: 31 August 2016

to separate them. As discussed in Section 2, the major ice nucleation is through the immersion freezing of DeMott et al. (2015), and with a specification that the largest droplets freeze first when ice nucleation occurs. Therefore, most of the newly-formed ice particles should be large and fall into the snow bins, and so N_s and Q_s contribute more significantly to ice number and mass increase with the increase of CCN than do N_i and Q_i. As CCN increases, not only cloud droplet number concentration (N_c) is increased, but also cloud mass mixing ratio (Q_c). The large increase of Q_c when CCN are high, which corresponds to the large increase of Q_s, will be scrutinized a little later. The decrease of raindrop number concentration and mass mixing ratio (N_r and Q_r, respectively) is very sharp and warm rain becomes negligible when INP are 1 cm^{-3} or larger (Fig. 3).

From the process rates of the major microphysical processes shown in Fig. 4, we see that the increase of Q_c with the increase of CCN and the decrease of Q_c with the increase of INPs are well explained by the condensation rate (Fig. 4a), although the changes of evaporation have the same trends as well. As shown in Figs. 4c and 4e, deposition is a more significant process than riming except in the case of extremely low INP (0.1 cm^{-3}) in this CMOC. Increasing CCN enhances deposition but only enhances riming when CCN are high. The sharp increase of deposition and riming rates from CCN1000 to CCN3000 explains the sharp increase of snow with a major contribution from deposition. How deposition and riming are enhanced so significantly in this case will be elucidated in Section 3.1.2

At the extremely low INPs of 0.1 cm^{-3}, the riming rate is similar to the deposition rate in this CMOC (Figs. 4c and 4e). As INPs increase, the contribution of riming is reduced significantly because of the reduction of supercooled droplets resulting from increased ice particles in the mixed-phase zone. Thus, the riming process is liquid-limited in this CMOC. As a

Atmos. Chem. Phys. Discuss., doi:10.5194/acp-2016-772, 2016
Manuscript under review for journal Atmos. Chem. Phys.
Published: 31 August 2016

Atmospheric Chemistry and Physics Discussions

result of increased ice particles, deposition is enhanced significantly, and it becomes 3-4 times larger than riming when INPs are 10 cm^{-3}. In the observed condition (i.e., CCN are between 30-300 cm^{-3} and INPs range between 1-10 cm^{-3}), both deposition and riming contribute to the snow growth but deposition is the major player. When INPs are extremely high (100 cm^{-3}), clouds glaciate very fast and liquid droplets that are available for riming are limited, therefore, its contribution is negligible (red line in Fig. 4e).

The Wegener–Bergeron–Findeisen (WBF) processes refer to ice depositional growth at the expense of liquid through evaporation in mixed-phase clouds. So the mixed-phase cloud regime where vapor pressure falls between the saturation vapor pressure over water and ice is defined as the WBF regime. As CCN increase, the WBF processes gets stronger as shown in Figs. 5a and 5b. The ratio of the evaporation through WBF to the total evaporation is larger than 0.92 in all simulations (Fig. 5a), meaning that drop evaporation in this CMOC occurs predominantly in the WBF regime. There is generally only 50-70% of deposition occurring in the WBF regime even when INP concentration is at 0.1 and 1 cm^{-3} (Fig. 5b), so a significant portion of deposition occurs outside of the WBF regime, and the portion increases as INP increase. Therefore, increasing INPs generally reduces the WBF regime because of the reduced liquid due to enhanced depositional growth. In this CMOC, the ratio of riming occurring in the WBF regime to the total riming is small (generally around 0.2-0.4 in Fig. 5c), meaning that riming mainly occurs outside of the WBF regimes under any CCN and INP conditions. The ratio is increased by CCN but generally decreased by INPs as a result of the increase/decrease of liquid regime, respectively (Fig. 5c).

We see that all major microphysical processes (condensation/evaporation, deposition/sublimation, and riming) are highly sensitive to INPs, while generally having much

Atmos. Chem. Phys. Discuss., doi:10.5194/acp-2016-772, 2016
Manuscript under review for journal Atmos. Chem. Phys.
Published: 31 August 2016

lower sensitivity to CCN when CCN are below 1000 cm^{-3}. The sensitivity of all the major microphysical processes to CCN gets much more significant when CCN are 1000 cm^{-3} and larger (Fig. 4), associated with significant changes in dynamics and thermodynamics and will be discussed in detail below.

3.1.2 Mechanism of enhanced snow precipitation by highly elevated CCN concentrations

Since the results of significant enhanced precipitation from CCN1000 to CCN3000 are unusual, besides verifying the use of identical initial and boundary meteorological conditions in all the experiments to eliminate simulation differences arising from inadvertent factors, we also conducted sensitivity tests by restoring the ice nucleation mechanisms to the default parameterizations (i.e., Meyers et al., 1992 for condensation/deposition and Bigg (1953) for immersing freezing) in the SBM but this yielded a similar conclusion. So, the significantly increased snow precipitation associated with elevated CCN concentrations is not the result of the particular ice-forming parameterization or the implementation approach of the parameterization.

Since the precipitation enhancement begins at 1400 UTC, which is a couple of hours into the simulations, we focus on the time period of 14-1600 UTC and use the simulations of different CCN concentrations with INP concentrations of 1 cm^{-3} to examine the mechanism. By taking a close look at ice nucleation (using model outputs every 6 min), we find that the total nucleated ice particle number concentration is increased as CCN increase and there is a large jump from CCN1000 to CCN3000 (Fig. 6a). The increase is caused by more cloud points that have ice nucleation occurring (Fig. 6b) and the enhanced nucleation rate (i.e., the nucleated ice particles per liter air volume within a hour) in the lower altitudes (Fig. 6c). Considering that the major ice formation mechanism is immersion freezing in this study, which requires the existence

Atmos. Chem. Phys. Discuss., doi:10.5194/acp-2016-772, 2016
Manuscript under review for journal Atmos. Chem. Phys.
Published: 31 August 2016

of drops for primary nucleation of ice, it means that there is much more supercooled liquid cloud area/volume available for nucleation in the lower altitudes as CCN increase (Fig. 6e). As shown in Fig. 6d, the increase of cloud water (Q_c) that is supercooled, since the warmest cloud temperature is below 0°C in this case, is very significant, with a big jump from CCN1000 to CCN3000, corresponding to the large increase of snow precipitation. From CCN1000 to CCN3000, the increase of the supercooled liquid area is especially drastic (Fig. 6e).

What causes the drastic increase of Q_c and a more widespread supercooled liquid cloud regime that is available for ice nucleation? We know that the increased drop surface area with the increased CCN can increase condensation, but it cannot explain such a drastic increase of the condensation rate averaged over the entire domain as shown in Fig. 6f. We find that over the domain the updraft area (i.e., grid points with w >1 m s^{-1}) is increased significantly with CCN with a jump from CCN1000 to CCN3000 as well (Fig. 7a), but the averaged updraft velocity does not change significantly (Fig. 7b), suggesting that much more convection occurs to form more clouds in the domain as CCN increase, especially in CCN3000. From the spatial distribution, we see that the increase of clouds is the most prominent around the valley and foothills (i.e., the lower-part of the windward slope of the Mountains). The cross sections of cloud water, rain and ice/snow mass mixing ratios at 1400 UTC clearly show that more clouds form over the valley and foothills in CCN3000, while in CCN30 clouds over the valley are fewer and clouds are shallower over the valley and foothills (Fig. 8a). we see much more invigorated mixed-phase clouds in CCN3000 compared with CCN30. The mixed-phase clouds start from the foothills in CCN3000 (Fig. 8c), while CCN30 does not have the mixed-phase clouds present until the regions above the middle and upper part of the mountain slope. This explains the increased ice nucleation rate at the lower altitudes as shown in Fig. 6c.

Changes of cloud fields described above must involve dynamic and thermodynamic changes. By examining the differences of dynamic and thermodynamic fields between CCN3000 and CCN30 (Fig. 9), we clearly see that a band of increased water vapor and relative humidity (RH) from the valley/foothills to the mountain at the higher altitudes (Fig. 9a-b). The corresponding temperature is only slightly decreased (Fig. 9c), which should not much affect the saturation water pressure and ice nucleation efficiency by much. So, the increased RH is mainly caused by the increased water vapor, and this increase can be up to 8% in RH (e.g., from RH of 70% to 78%). The large increase of Q_v and RH is mainly a result of changed local circulation as shown in Figs. 9d-e: the wind blowing to windward slope (zonal wind) gets stronger from CCN30 to CCN3000 (within ~ 2 km above the ground) over the slope. In the cases of atmospheric rivers, the stronger zonal wind transport means an increase of moisture transport to the Mountains.

The changes of winds are only significant at the slope of the Mountains and occur only after 2 h of the simulations (Fig. 10a), suggesting that it stems from more latent heat release as a result of more clouds over the valley and foothills (feedbacks of radiation and precipitation take much longer time especially considering the two-hour time is 4- 6 am LST). The clouds at the valley/foothills locations are generally shallow. Many literature studies, including both observations and model simulations, have shown that CCN enhance shallow cloud formation and deepen shallow clouds (e.g., Chen et al. 2015; Yuan et al. 2011; Pincus and Baker 1994; Koren et al. 2014), which can be due to various reasons such as cloud lifetime effect, enhanced turbulent convection by larger entrainment rates as a result of stronger evaporation, and greater latent heat release due to larger drop surface area for stronger condensation. We find that condensation is indeed much enhanced over the valley/foothills from CCN30 to CCN3000 with

INP of 1 cm^{-3} (Fig. 9f), which results in much reduced supersaturation with respect to water (supersaturation around the cloud base in CCN30 at 1300 UTC is about 0.28% while only 0.04% in CCN3000). The enhanced condensation as well as the cloud lifetime effect (i.e., conversion of smaller droplets into rain is slow and cloud can be sustained for a longer time) contributes to more shallow clouds at the valley/foothills. The more latent heat resulting from enhanced condensation leads to the change of local circulation, which transports more moisture to the windward slope of the Mountain,resulting in more active mixed-phase clouds and snow precipitation through enhanced deposition and riming. In addition, over the Mountains more supercooled liquid would be lifted to the higher altitudes in the polluted condition, forming ice/snow more efficiently through immersion freezing at the colder temperature, which contributes to more snow precipitation as well.

It should be noted that the mixed-phase clouds over the Mountains are the key to the enhanced precipitation by CCN. In the sensitivity tests based on the WMOC case where ice-related microphysics is turned-off (the WMOC case is chosen because ice processes are weak), precipitation is dramatically suppressed from CCN of 30 cm^{-3} to 3000 cm^{-3} (Fig. 11a) and there is almost no precipitation at the valley and windward slope in CCN3000 due to extremely small droplets. However, we still see the change of the local circulation over the slope as a result of enhanced condensation (Fig. 11b). Therefore, presence of ice is a necessary condition for such a large increase precipitation by CCN. Without ice processes (e.g., under the warm season with warm clouds only), precipitation over the Mountains can not form efficiently in such a polluted condition even with the increased moisture. But the added latent heat from condensation of vapor to water is still the main energy source of the invigoration.

In summary, increasing CCN forms more clouds at the valley and foothills (generally

Atmos. Chem. Phys. Discuss., doi:10.5194/acp-2016-772, 2016
Manuscript under review for journal Atmos. Chem. Phys.
Published: 31 August 2016

Atmospheric Chemistry and Physics
Discussions

shallow) through much enhanced condensation, which induces a local circulation change due to more latent heat release that enhances the zonal transport of moisture, leading to the invigoration of the orographic mixed-phase clouds and drastically increased snow precipitation in this CMOC case. Therefore, aerosol impacts on orographic mixed-phase clouds can be extraordinary in extremely polluted conditions, especially under the influence of atmospheric rivers. Besides the the key role of ice processes for leading to greatly enhanced precipitation, orographic dynamics is another important factor since we do not see such impacts in the sensitivity tests where the terrain height is set to be 600 m for the locations with a terrain height > 600 m (precipitation becomes very small in those sensitivity tests and the increase from CCN30 to CCN3000 is small as well).

The increases of Q_v and RH are the most significant from CCN1000 to CCN3000 due to non-linearity of aerosol-cloud interactions, explaining the large increase of snow precipitation. It is worth noting in CCN3000, warm rain is completely shut off (left column in Fig. 8b), therefore, much more cloud water can be transported to higher altitudes for more immersion freezing, which further enhances the snow precipitation. This likely contributes to the steep increase in precipitation when CCN reach 3000 cm^{-3}.

3.1.3 Supercooled water content (SCW) and cloud phase

Through changing the microphysical process rates, CCN and INP impact the cloud phases and supercooled water content (SCW). Fig. 12 shows that INPs have the most striking impact on SCW. Increasing INPs enhances ice particle formation, and then facilitates the deposition and riming processes in this CMOC as discussed in Section 3.1.1. The enhanced deposition in the WBF regime, along with riming, leads to a faster conversion of liquid to ice in the mixed-phase and glaciates the clouds faster. Therefore, SCW is substantially reduced as INPs increase (Fig. 12a). For example, in the case of CCN300, a significant amount of liquid mass fraction (0.1) exists at the temperature of -30°C when INP is 0.1 cm^{-3}. Such temperature is increased to -20, and -10°C as INPs are increased to 1 and 10 cm^{-3}, respectively. In the extremely high INP case (100 cm^{-3}), there is nearly no supercooled water. As a result, the fractions of cloud phases are dramatically changed (Fig. 13a). As expected, higher INP concentrations decreases the fractions of liquid and mixed phases due to increasing the fraction of ice phase. In this CMOC, the cloud phases are most sensitive to INPs at relatively low concentrations. For example, when INPs increase from 0.1 to 1 cm^{-3}, which is likely common for this region based on observations in the past field campaigns, the liquid phase fraction is reduced by nearly half and the ice phase fraction is increased by 2 times or larger (Fig. 13a). Note that the effects of INPs on cloud phase and SCW presented in this study may represent the upper limit because ice formation is mainly through immersion freezing that transforms the large liquid particles to ice particles when ice forms.

Compared with the effects of INPs, the magnitudes of CCN effects on SCW and cloud phases are much smaller but still significant (the lines with same color but different line styles in Fig. 12). Moreover, the sign is opposite. Increasing CCN generally increases SCW slightly (Figs. 12a). The impact of CCN on cloud phases is generally small, except when INPs are very low, i.e., at 0.1 cm^{-3} (Figure 13a). In this low INP case, increasing CCN increases ice phase fractions and reduces the mixed-phase fraction when CCN are relatively low. This is because liquid clouds are dominant so such clouds are sensitive to the CCN-enhanced ice nucleation as discussed in the section 3.1.2.

Atmos. Chem. Phys. Discuss., doi:10.5194/acp-2016-772, 2016
Manuscript under review for journal Atmos. Chem. Phys.
Published: 31 August 2016

3.2 WMOC – MAR02

For this warm mixed-phase cloud case, the surface accumulated precipitation is suppressed by increasing CCN when CCN are lower than 1000 cm^{-3} (Fig. 14a), which is different from the case of CMOC where the sign of CCN impact on precipitation depends on INP concentration. This is because the clouds in this WMOC behave similarly as warm clouds due to less efficient ice nucleation at the warm cloud temperatures. When CCN are lower than 1000 cm^{-3}, the large decrease of warm rain (Fig. 14b) overpowers the slight changes of snow precipitation (Fig. 14c). Similar to the CMOC case, we see a drastic increase of surface precipitation from CCN1000 to CCN3000, also due to drastic increase of snow precipitation. Increasing INPs enhances surface precipitation in a more significant manner than that in CMOC. In other words, the WMOC is more sensitive to INPs than the CMOC.

The in-cloud microphysical properties also show similar results as for the CMOC: the steep increases of the snow mass and cloud water mixing ratios from CCN1000 to CCN3000 (Fig. 15). We have done the same investigation as in Section 3.1.1, and found the mechanism causing the increased cloud water and the snow production is similar as that in CMOC, that is, increasing CCN forms more shallow clouds at the large area of valley and foothills, which induces a change of local circulation significantly through more latent heat release, which in turn increases the zonal transport of moisture to the windward slope of the mountains. Additionally, more abundant warm rain is present at the wide valley area in this case when CCN is low (30 cm^{-3}) compared with the CMOC. The suppression of warm rain as CCN increase is very significant as shown in Figs. 14b and 15. Over the Mountain, this suppression increases Q_c and allows more cloud water to be transported to the higher altitudes along the slope where immersion freezing is able to occur at lower temperatures. Ice multiplication through the Hallet-Mossop parameterization (Hallet and Mossop, 1974) in this WMOC contributes to ice particle concentration by 10-15% when CCN are 30 cm^{-3} and INPs are 1 cm^{-3} in our model simulation with the fast version of SBM in which ice habits are not considered. Therefore, as more ice particles form from immersion freezing when CCN increase, the ice multiplication processes would further increase ice crystal formation although the contribution is relatively small in the model simulation. Past observation studies suggested that ice multiplication through rime-spintering does occur in the orographic mixed-phase clouds of this region (Marwitz 1987; Rauber 1992). We do not yet have a clear understanding of the importance of this process in contributing to ice formation in reality. After more ice particles form, the subsequent ice depositional and riming growth processes form efficient snow precipitation. The CCN impact on local circulation change is more significant in this case compared with the CMOC, probably due to much more shallow warm clouds in the valley.

Different from the CMOC case, riming is a more efficient ice growth process to form snow than deposition in this case except when INP concentrations are extremely high (100 cm^{-3}) where both riming and deposition contribute in a similar magnitude (Fig. 16). In addition, the riming rate is increased as INP concentrations increase, which is opposite to that of CMOC. This is because the WMOC is ice-limited and there are not enough ice particles to collide with liquid particles when INP numbers are low, therefore, increasing INPs boosts ice particles and allows more riming to occur. In contrast, the CMOC case is liquid-limited, so increasing INPs reduces liquid particles available for riming due to ice depositional growth. We also see that condensation and evaporation rates are generally more than 2 times larger in this case compared with CMOC and both rates increase more significantly with CCN concentration in this WMOC. This is related to the dominance of liquid clouds in the WMOC. The more significant increase of condensation by increasing CCN compared with the CMOC is likely a result of the more significant change of the local circulation that is associated with more shallow clouds forming at the valley. Increasing INP number concentrations reduces evaporation simply because of the reduction of liquid due to the increased deposition and riming.

Similarly as in the CMOC, increasing CCN enhances the WBF process for this WMOC as more droplet evaporation and ice deposition occur (Figs. 17a and 17b). With the increase of CCN, the domain-mean riming rate is not changed much until CCN of 1000 cm^{-3} (Fig. 16e), but the riming rate in the WBF regime is increased (Fig. 17c), possibly due to larger ice particles resulting from stronger deposition growth in the WBF regime.

Similar results regarding CCN and INP impact on supercooooled water content are obtained in the WMOC case as in the CMOC case: increasing INPs dramatically reduces SCW and increases cloud glaciation temperature, while increasing CCN has the opposite effect with much smaller significance (Fig. 12b). Compared with the CMOC, the effects of INP on SCW are a little smaller but CCN effects are a little larger. The liquid phase fraction (number fraction of cloudy grid points for which the liquid represents 99% or more of the condensate mass) decreases significantly as INPs increase (Fig. 13b). Correspondingly the fractions of the mixed-phase and ice phase cloud volumes increase due to increased ice nucleation. Similar to the increased riming as INPs increase, the mixed-phase fraction is increased as well in the WMOC, which is opposite to the case for CMOC, as a result of the ice-limited condition in the WMOC versus the liquid-limited condition in the CMOC. Note that INP effects are more significant at higher INP concentrations in this case, while in CMOC the sensitivity decreases as INP increases, suggesting that the optimal INP concentration for the maximum INP impact is higher in warmer clouds than the colder clouds, because of less efficient ice formation at the warmer cloud temperatures. The CCN impacts on cloud phase are more significant in this WMOC compared with those in CMOC. The decreased liquid cloud fraction with the increase of CCN is a consequence of the large increase of ice phase fraction resulting from more active cold-cloud processes, since the total cloud fraction sums up to 1 (Fig. 13b).

4. Conclusions and Discussion

Extending the previous study of Fan et al. (2014), we conducted new simulations at higher resolution and further sensitivity studies based around the same two mixed-phase orographic clouds forming on the Sierra Nevada barrier under the influence of atmospheric rivers that were our focus from the CalWater 2011 field campaign, to quantify the response of precipitation to changes of CCN and INP and to examine CCN and INP impacts on SCW and cloud phases. The two mixed-phase cloud cases have contrasting thermodynamics and dynamics: FEB16 has cold cloud temperatures and northwesterly wind flow at lower-levels (i.e., CMOC), while MAR02 has about 10 °C warmer cloud temperatures and southerly wind flow (i.e., WMOC).

It is found that, in the CMOC case, deposition contributes more significantly to snow production than the riming because deposition process is efficient at the cold cloud temperatures (from -22 to -32 °C) in this case. In the WMOC, riming generally contributes more significantly because the deposition growth process is less efficient at the warmer temperatures (generally warmer than -20 °C in this case), except in the extremely high INP case where both riming and deposition contribute similarly.

We find that increasing INP concentrations enhances snow precipitation on the windward slope of the Sierra Nevada Mountains in both CMOC and WMOC cases. With the increase of

INPs, the increased ice nucleation via immersion freezing enhances snow formation by intensifying depositional growth of ice in the CMOC while both deposition and riming contribute in the WMOC. Increasing INPs reduces riming in the CMOC, because of the liquid-limited condition in which more efficient depositional growth at higher INP number concentrations glaciates clouds and reduces liquid particles available for riming. However, in the ice-limited conditions of WMOC, increasing INPs boosts ice particle concentrations so that more riming can occur in a liquid-rich condition. For the same reason, increasing INPs suppresses the WBF processes due to reduced liquid particles.

The CCN impacts on precipitation are complicated, depending on cloud temperature, and concentrations of CCN and INP. When CCN are lower than 1000 cm^{-3}, boosting CCN concentrations slightly increases snow precipitation, but the total precipitation can be increased or decreased depending on INP concentrations in the CMOC. In contrast, in the WMOC, increasing CCN suppresses the total precipitation due to the large suppression of warm rain production. We find a drastic increase of snow precipitation by increasing CCN when CCN are high (1000 cm^{-3} or larger), consistently in both CMOC and WMOC, as a result of increased deposition and riming rates. The mechanism by which this occurs is through increasing CCN forming more shallow clouds at the wide valley area and foothills, which induces a change of local circulation through more latent heat release and increases the zonal transport of moisture to the windward slope of the Mountains. This results in much more invigorated mixed-phase clouds with enhanced deposition and riming processes and therefore much more snow precipitation. Additionally, over the mountains, the suppression of warm rain as CCN increase allows more cloud droplets to be transported to the higher altitudes where immersion freezing is able to occur efficiently, contributing to the enhanced snow as well. This effect is most significant when warm rain is completely shut off at CCN of 1000 cm^{-3} and higher.

Increasing INP concentrations dramatically reduces supercooled water content and increases cloud glaciation temperature, while increasing CCN has the opposite effect but with much smaller significance. As expected, the fraction of liquid phase clouds is decreased and the ice phase fraction is increased by increasing INP in both cases. However, we see a decreased fraction of mixed-phase clouds by INP in the CMOC but increased in the WMOC, relating to the liquid-limited condition in the former where increasing ice formation enhances cloud glaciation, while the ice-limited condition in the latter in which more liquid clouds are converted to mixed-phase clouds as INPs increase. Compared with the effects of INPs, the magnitudes of CCN effects on SCW and cloud phases are much smaller and the signs are opposite. Increasing CCN generally enhances SCW in both cases. The relative fractions of cloud phases are not much impacted by CCN in the CMOC, except when INP is very low (i.e., 0.1 cm^{-3}). However, in the WMOC, increasing CCN evidently decreases liquid cloud fraction but increases ice phase fraction. Thus, cloud phases in the WMOC have a large sensitivity to CCN compared with CMOC.

This study provides a better understanding of the CCN and INP effects on orographic mixed-phase cloud properties and precipitation. The result that CCN dramatically increase snow precipitation over the mountains when CCN are high (l000 cm^{-3} or larger) as a result of modified cloud properties at the valley and foothills is different from previous modeling studies in the literature. The mechanism for the drastic increase of the snow precipitation by CCN at the very polluted condition is new, and it suggests a strong impact of the shallow clouds at the valley and foothills on the mixed-phase clouds and precipitation over the mountains. It is worthy noting that we do not see such a significantly increased precipitation by CCN in the sensitivity tests without ice-related processes or without topography, suggesting that ice processes in the mixed-phase clouds and orographically-forced dynamics are the key factors for such CCN effects.

Over the region of Sierra Nevada Mountains, CCN of above 1000 cm^{-3} would be an extreme condition. Therefore, this mechanism would not occur usually and the change of precipitation would not be much when CCN is less than 1000 cm^{-3} as shown in Fig. 2a and 14a in the normal conditions over this region. It is shown precipitation suppression by CCN in the relatively warm situations, in agreement with the observations of Rosenfeld and Givati (2006). However, for many polluted regions such as China and India where CCN of above 1000 cm^{-3} are quite common, this mechanism may have very important implications for orographic precipitation extremes and water cycles.

It should be noted that the results of CCN and INP impacts on the precipitation and supercooled water content may represent an upper limit since the major ice nucleation in the simulations is through immersion freezing that converts largest liquid drops into ice or snow directly when ice nucleation occurs, leading to very efficient conversion of liquid to ice/snow and then strong ice growth processes to form snow.

In our study, we do not see significant spillover effect of snowfall (i.e., decrease at the windward slope and increase at the leeside slope by increasing CCN) as found in Saleeby et al. (2011). Precipitation mainly forms on the windward slope of the Sierra Nevada Mountains and the increase of the snow precipitation is more significant on the windward slope than on the lee side in both cases. The different results between our study and Saleeby et al. (2011) could be related to different locations of the clouds over the mountain and/or different mountain topography, or the presence of a low-level barrier jet in the atmospheric river environment that reduces the cross barrier flow.

Acknowledgements

This study was supported by the California Energy Commission (CEC) and the Office of Science of the U.S. Department of Energy as part of the Regional and Global Climate Modeling program. PNNL is operated for DOE by Battelle Memorial Institute under Contract DE-AC06-76RLO1830.

References

Ault, A. P., Williams, C. R., White, A. B., Neiman, P. J., Creamean, J. M., Gaston, C. J., Ralph, F. M., and Prather, K. A.: Detection of Asian dust in California orographic precipitation, J. Geophys. Res., 116, D16205, doi:10.1029/2010JD015351, 2011.

Bao, J.-W., Michelson, S. A., Neiman, P.J., Ralph, F. M., and Wilczak, J. M.: Interpretation of enhanced integrated water vapor bands associated with extratropical cyclones: Their formation and connection to tropical moisture, Mon. Wea. Rev., 134, 1063-1080, doi:10.1175/MWR3123.1, 2006.

Cesana, G., and Chepfer, H.: Evaluation of the cloud thermodynamic phase in a climate model using CALIPSO-GOCCP, J. Geophys. Res. Atmos., 118, 7922–7937, doi:10.1002/jgrd.50376, 2013.

Chen, Y.-C., Christensen, M. W., Diner, D. J., and Garay, M. J.: Aerosol-cloud interactions in ship tracks using Terra MODIS/MISR: J, Geophys. Res., 120, 2819-2833, doi:10.1002/2014jd022736, 2015.

Cotton, W., Tripoli, G., Rauber, R., and Mulvihill, E.: Numerical simulation of the effects of varying ice crystal nucleation rates and aggregation processes on orographic snowfall, J. Climate Appl. Meteor., 25, 1658–1680, 1986.

Creamean, J. M., Suski, K. J., Rosenfeld, D., Cazorla, A., DeMott, P. J., Sullivan, R. C., White, A. B., Ralph F. M., Minnis P., Comstock, J. M., Tomlinson, J, M., and Prather, K. A.: Dust and Biological Aerosols from the Sahara and Asia Influence Precipitation in the Western U.S., Science, 339, 1572-1578, DOI: 10.1126/science.1227279, 2013..

DeMott, P. J., Prenni, A. J., McMeeking, G. R., Tobo, Y., Sullivan, R. C., Petters, M. D., Niemand M., Möhler, O., and Kreidenweis, S. M.: Integrating laboratory and field data to quantify the immersion freezing ice nucleation activity of mineral dust particles, *Atmos. Chem. Phys.,* 15, 393–409, 2015.

Fan, J., Leung, L. R., DeMott, P. J., Comstock, J. M., Singh, B., Rosenfeld, D., Tomlinson, J. M., White, A., Prather, K., Minnis, P., Ayers, J. A., and Min, Q.: Aerosol Impacts on California Winter Clouds and Precipitation during CalWater 2011: Local Pollution versus Long-Range Transported Dust, Atmos. Chem. Phys., 14, 81-101, 2014.

Atmos. Chem. Phys. Discuss., doi:10.5194/acp-2016-772, 2016
Manuscript under review for journal Atmos. Chem. Phys.
Published: 31 August 2016

Atmospheric Chemistry and Physics Discussions

Fan, J., Leung, L. R., Li, Z., Morrison, H., Chen, H., Zhou, Y., Qian, Y., and Wang, Y.: Aerosol impacts on clouds and precipitation in eastern China: Results from bin and bulk microphysics, J. Geophys. Res., 117, D00K36, doi:10.1029/2011JD016537, 2012.

Fan, J., Ovtchinnikov, M., Comstock, J., McFarlane, S. A., and Khain, A.: Ice Formation in Arctic Mixed-Phase Clouds - Insights from a 3-D Cloud-Resolving Model with Size-Resolved Aerosol and Cloud Microphysics, J. Geophys. Res., 114, D04205, doi:10.1029/2008JD010782, 2009.

Fan, J., Zhang, R., Li, G., and Tao, W.-K.: Effects of aerosols and relative humidity on cumulus clouds, J. Geophys. Res., 112, D14204, doi:10.1029/2006JD008136, 2007.

Fridlind, A. M., Ackerman, A. S., McFarquhar, G., Zhang, G., Poellot, M. R., DeMott, P. J., Prenni, A. J., and Heymsfield, A. J.:, Ice properties of single-layer stratocumulus during the Mixed-Phase Arctic Cloud Experiment: 2. Model results, J. Geophys. Res., 112, D24202, doi:10.1029/2007JD008646, 2007.

Hallett, J., and S. C. Mossop: Production of secondary ice particles during the riming process, Nature, 249(5452), 26-28, 1974.

Ilotoviz E., Khain, A. P., Benmoshe, N., Phillips, V. T. J., and Ryzhkov, A.V.: Effect of Aerosols on Freezing Drops, Hail, and Precipitation in a Midlatitude Storm, Journal of the Atmospheric Sciences, 73(1), 109-144, 2016.

Jirak, I. L., and Cotton, W. R.: Effect of air pollution on precipitation along the Front Range of the Rocky Mountains, J. Appl. Meteor. Climatol., 45, 236–245, 2006.

Kay, J. E., Bourdages, L., Miller, N. B., Morrison, A., Yettella, V., Chepfer, H., and Eaton B., Evaluating and improving cloud phase in the Community Atmosphere Model version 5 using spaceborne lidar observations, J. Geophys. Res. Atmos., 121, doi:10.1002/2015JD024699, 2016.

Khain, A. P., Pokrovsky, A., Pinsky, M., Seifert, A., and Phillips, V.: Simulation of effects of atmospheric aerosols on deep turbulent convective clouds using a spectral microphysics mixed-phase cumulus cloud model. Part I: Model description and possible applications, J. Atmos. Sci., 61, 2963–2982, 2004.

Khain, A., Leung. L. R., Lynn, B., and Ghan, S.: Effects of aerosols on the dynamics and microphysics of squall lines simulated by spectral bin and bulk parameterization schemes, J. Geophys. Res., 114, D22203, doi:10.1029/2009JD011902, 2009.

Koren, I., Dagan G., and Altaratz O.: From aerosol-limited to invigoration of warm convective clouds. Science, 344, 1143-1146, doi:10.1126/science.1252595, 2014.

Li, G., Wang, Y., and Zhang, R.: Implementation of a two-moment bulk microphysics scheme to the WRF model to investigate aerosol-cloud interaction, J. Geophys. Res., 113, D15211, doi:10.1029/2007JD009361, 2008.

Lowenthal, D. H., Borys, R. D., Cotton, W., Saleeby, S., Cohn, S. A., and Brown, W. O. J.: The altitude of snow growth by riming and vapor deposition in mixed□phase orographic clouds, Atmos. Environ., 45(2), 519–522, doi:10.1016/j.atmosenv.2010.09.061, 2011.

Lynn, B., Khain, A., Rosenfeld, D., and Woodley, W. L.: Effects of aerosols on precipitation from orographic clouds, J. Geophys. Res., 112, D10225, doi:10.1029/2006JD007537, 2007.

Marwitz, J. D., Deep Orographic Storms over the Sierra Nevada. Part II: The Precipitation Processes, J. Atmos. Sci., 44(1), 174–185, 1987.

Meyers, M. P., DeMott, P. J., and Cotton, W. R.: New primary ice-nucleation parameterizations in an explicit cloud model, J. Appl. Meteor., 31, 708–721, 1992.

Muhlbauer, A., and Lohmann, U.: Sensitivity studies of aerosol cloud interactions in mixed-phase orographic precipitation, J. Atmos. Sci., 66(9), 2517–2538, doi:10.1175/2009JAS3001.1., 2009.

Neiman, Paul J., Sukovich, E. M., Ralph, F. M., Hughes, M.: A Seven-Year Wind Profiler–Based Climatology of the Windward Barrier Jet along California's Northern Sierra Nevada. Mon. Wea. Rev., 138, 1206–1233, 2010.

Pincus, R., and Baker, M. B.: Effect of Precipitation on the Albedo Susceptibility of Clouds in the Marine Boundary-Layer. Nature, 372, 250-252, doi: 10.1038/372250a0, 1994.

Ralph, F. M., Neiman, P. J., Kiladis, G. N., Weickman, K., and Reynolds, D. W.: A multi-scale observational case study of a Pacific atmospheric river exhibiting tropical-extratropical connections and a mesoscale frontal wave. Mon. Wea. Rev., 139, 1169-1189, doi:10.1175/2010MWR3596.1 , 2011.

Rauber, R.: Microphysical Structure and Evolution of a Central Sierra Nevada Orographic Cloud System, J. Appl. Meteor., 32, 3-24, 1992.

Rosenfeld, D., and Givati, A.: Evidence of orographic precipitation suppression by air pollution-induced aerosols in the western United States, J. Appl. Meteorol. Climatol., 45(7), 893–911, doi:10.1175/JAM2380.1., 2006.

Atmospheric Chemistry and Physics Discussions

Rosenfeld, D., Lohmann, U., Raga, G. B., O'Dowd, C. D., Kulmala, M., Fuzzi, S., Reissell, A., and Andreae, M. O.: Flood or drought: How do aerosols affect precipitation?, Science, 321, 1309 – 1313, doi:10.1126/science.1160606, 2008.

Rosenfeld, D., Yu, X., Liu, G., Xu, X., Zhu, Y., Yue, Z., Dai, J., Dong, Z., Dong, Y., and Peng, Y.: Glaciation temperatures of convective clouds ingesting desert dust, air pollution and smoke from forest fires, Geophys. Res. Lett., 38, L21804, doi:10.1029/2011GL049423, 2011

Rosenfeld, D., Rei, Chemke, DeMott, P., Sullivan, R. C., Rasmussen, R., McDonough, F., Comstock, J., Schmid, B., Tomlinson, J., Jonsson, H., Suski, K., Cazorla, A., and Prather, K., The common occurrence of highly supercooled drizzle and rain near the coastal regions of the western United States, J. Geophys. Res. Atmos., 118, doi:10.1002/jgrd.50529, 2013.

Saleeby, S. M., Cotton, W. R., and Fuller, J. D. The Cumulative Impact of Cloud Droplet Nucleating Aerosols on Orographic Snowfall in Colorado, Journal of Applied Meteorology and Climatology, 50(3), 604-625, 2011.

Saleeby, S. M., Cotton, W. R., Lowenthal, and Messina, J.: Aerosol Impacts on the Microphysical Growth Processes of Orographic Snowfall, J. Appl. Meteorol. Climatol., 52, 834–850, 2013.

Shen, X., Wang, Y., Zhang, N., and Li, X.: Precipitation and cloud statistics in the deep tropical convective regime, J. Geophys. Res., 115, D24205, doi:10.1029/2010JD014481, 2010.

Tao, W.-K., Chen, J.-P., Li, Z., Wang, C., and Zhang, C.: Impact of aerosols on convective clouds and precipitation, Rev. Geophys., 50, RG2001, doi:10.1029/2011RG000369, 2012.

Uno, I., Eguchi, K., Yumimoto, K., Takemura, T., Shimizu, A., Uematsu, M., Liu, Z., Wang, Z., Hara, Y., and Sugimoto, N.: Asian dust transported one full circuit around the globe, Nat. Geosci., 2(8), 557–560, doi:10.1038/ngeo583, 2009.

Xiao, H., Yin, Y., Jin, L., Chen, Q., and Chen, J.: Simulation of the effects of aerosol on mixed-phase orographic clouds using the WRF model with a detailed bin microphysics scheme, J. Geophys. Res. Atmos., 120, 8345–8358, doi:10.1002/ 2014JD022988, 2015.

Young, K. C.: A numerical simulation of wintertime, orographic precipitation. Part I: Description of model microphysics and numerical techniques. J. Atmos. Sci., 31,1735–1748, 1974.

Yuan, T., Remer, L. A., and Yu, H.: Microphysical, macrophysical and radiative signatures of volcanic aerosols in trade wind cumulus observed by the A-Train. Atmos. Chem. Phys, 11, 7119-7132, 2011.

Zipori, A., Rosenfeld, D., Tirosh, O., Teutsch, N., and Erel, Y.: Effects of aerosol sources and chemical compositions on cloud drop sizes and glaciation temperatures, J. Geophys. Res. Atmos., 120, 9653–9669, doi:10.1002/2015JD023270, 2015

Atmos. Chem. Phys. Discuss., doi:10.5194/acp-2016-772, 2016
Manuscript under review for journal Atmos. Chem. Phys.
Published: 31 August 2016

Atmospheric Chemistry and Physics
Discussions

Table 1 Model simulations that are run for different CCN and dust concentrations. Please note that INP denotes dust/bio particle number concentration with particle size > 0.5 μm for use in the parameterization of DeMott et al. (2015), as described in FAN2014.

		INP (cm^{-3})			
		0.1	1	10	100
CCN (cm^{-3})	30	x	x	x	x
	100	x	x	x	x
	300	x	x	x	x
	1000	x	x	x	x
	3000	x	x	x	x

Atmos. Chem. Phys. Discuss., doi:10.5194/acp-2016-772, 2016
Manuscript under review for journal Atmos. Chem. Phys.
Published: 31 August 2016

Atmospheric Chemistry and Physics Discussions
Open Access

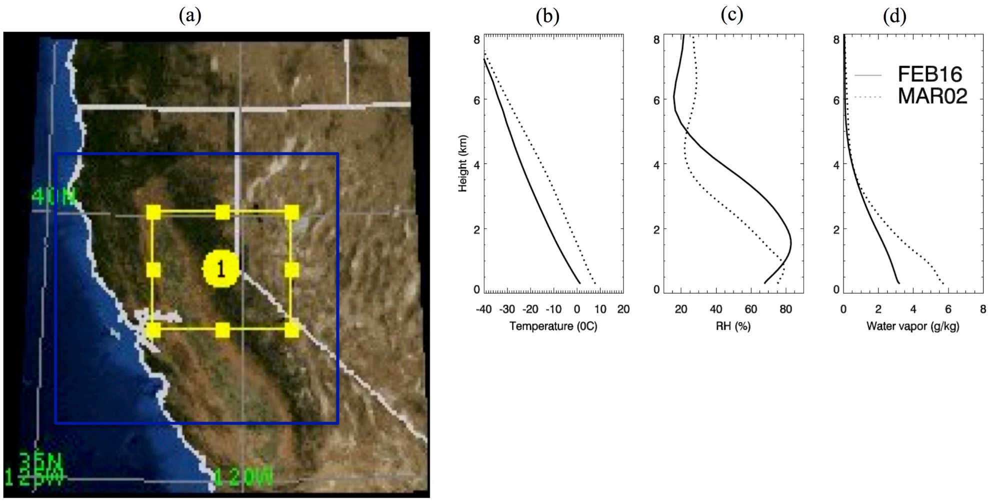

Fig. 1 (a) The simulation domain (yellow box), and the vertical profiles of (b) the temperature, (c) RH, and (d) water vapor for CMOC (FEB16) and WMOC (MAR02). (b)-(d) are domain mean values during the model simulation time period. The blue box in (a) denotes the domain of 2 km resolution simulations done in FAN2014.

Atmos. Chem. Phys. Discuss., doi:10.5194/acp-2016-772, 2016
Manuscript under review for journal Atmos. Chem. Phys.
Published: 31 August 2016

Atmospheric Chemistry and Physics
Open Access
Discussions

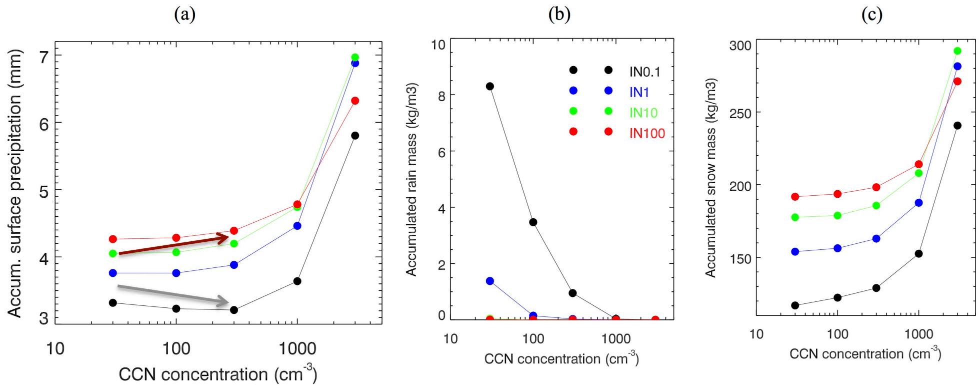

Fig. 2 (a) The domain-mean accumulated surface precipitation, and the accumulated (b) rain and (c) snow mass concentrations at the lowest model level (~ 40 m above the surface) during the simulation time period for CMOC. All domain- mean calculation excludes the lateral boundary grid points in this study.

Atmos. Chem. Phys. Discuss., doi:10.5194/acp-2016-772, 2016
Manuscript under review for journal Atmos. Chem. Phys.
Published: 31 August 2016

Atmospheric Chemistry and Physics
Discussions

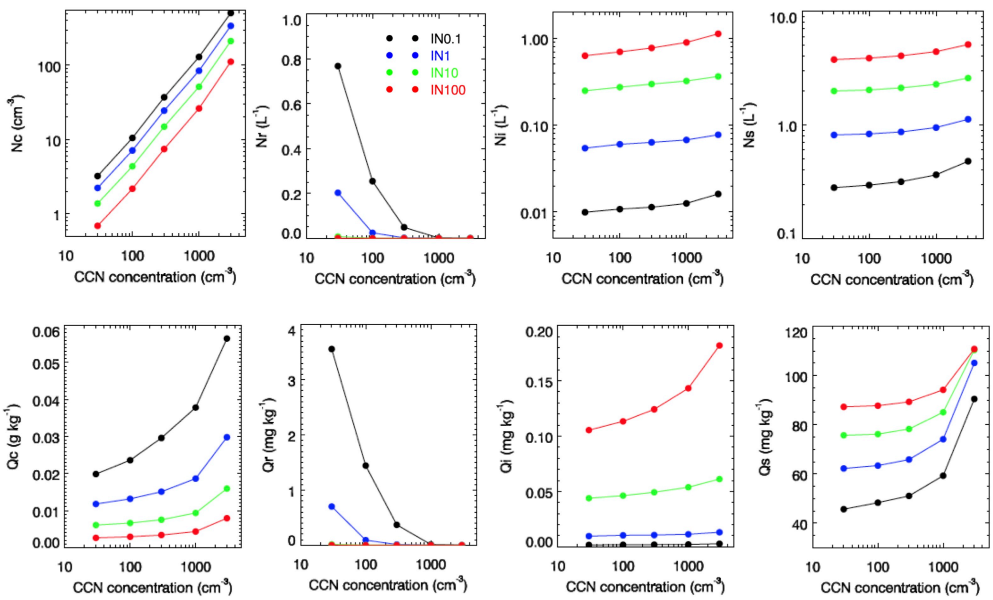

Fig. 3 The number concentrations (top row) and mass mixing ratios (bottom row) of droplet (1st column), rain (2nd column), cloud ice (3rd column), and snow (4th column) for CMOC. The data are averaged over the grid points over the domain by excluding the lateral boundary grid points below the 7 km altitude and over the simulation time by excluding the initial two hours.

Atmos. Chem. Phys. Discuss., doi:10.5194/acp-2016-772, 2016
Manuscript under review for journal Atmos. Chem. Phys.
Published: 31 August 2016

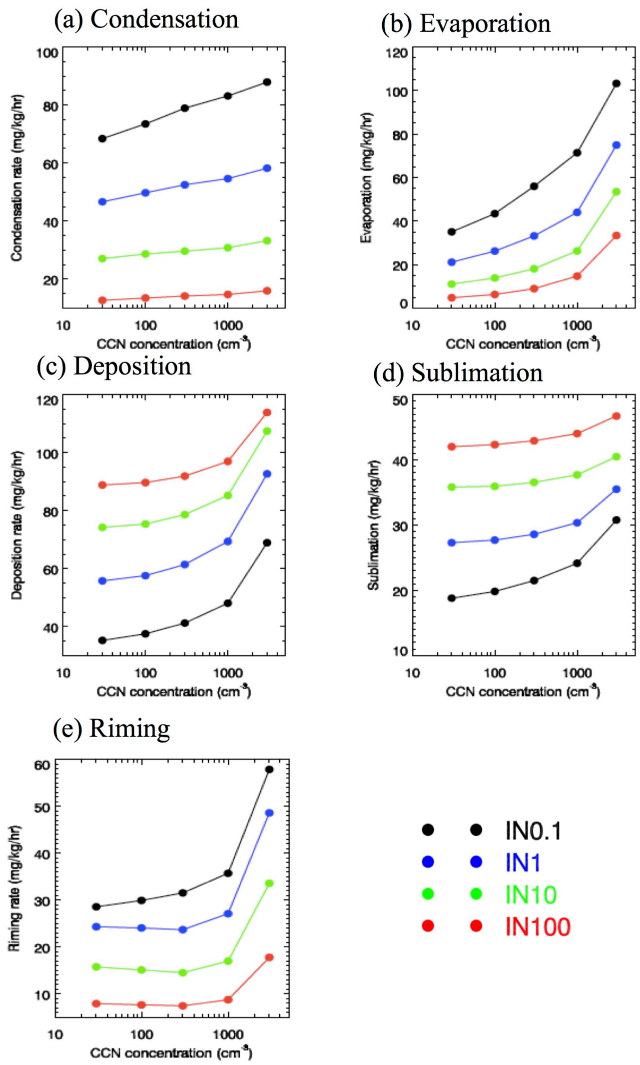

Fig. 4 The microphysical process rates of (a) condensation, (b) evaporation, (c) deposition, (d) sublimation, and (e) riming for CMOC. The model outputs for the process rates are in every 6 min frequency, and the data shown in the plots were processed in the same way as Fig. 3.

Atmos. Chem. Phys. Discuss., doi:10.5194/acp-2016-772, 2016
Manuscript under review for journal Atmos. Chem. Phys.
Published: 31 August 2016

Atmospheric Chemistry and Physics Discussions
Open Access

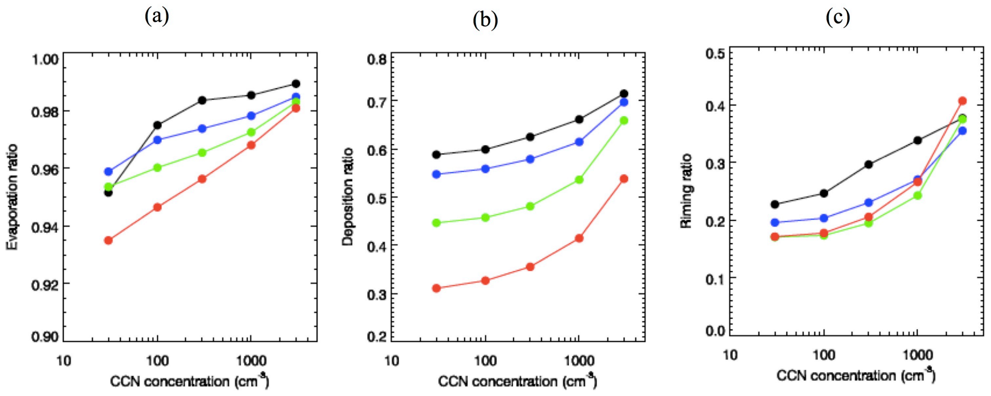

Fig. 5 (a) The ratio of evaporation occurring in the WBF regime that is defined as the grid points where the WBF processes occur) to the total evaporation for the CMOC case. (b) and (c) are the same as (a), except for deposition and riming, respectively. Data were processed in the same way as Fig. 3.

Atmos. Chem. Phys. Discuss., doi:10.5194/acp-2016-772, 2016
Manuscript under review for journal Atmos. Chem. Phys.
Published: 31 August 2016

Atmospheric Chemistry and Physics
Discussions

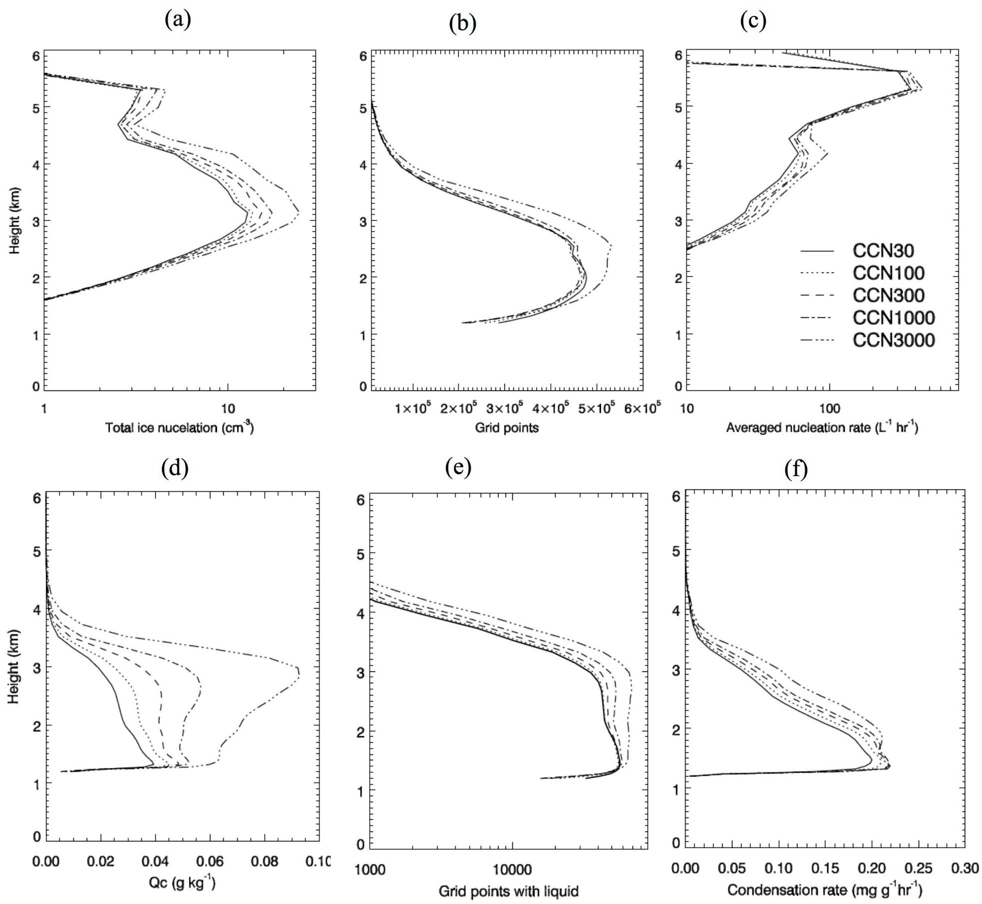

Fig. 6 Vertical profiles of (a) total nucleated ice particles, (b) the total grid points where ice nucleation occurs, (c) the ice nucleation rate averaged over the total ice nucleation grid points, (d) domain-mean cloud water content (Q_c), (e) the total grid points that have liquid (i.e., the liquid water mixing ratio is larger than 1.e-5 kg kg^{-1}), and (f) the domain-mean condensate rate during 1400-1600 UTC for the CMOC case.

Atmos. Chem. Phys. Discuss., doi:10.5194/acp-2016-772, 2016
Manuscript under review for journal Atmos. Chem. Phys.
Published: 31 August 2016

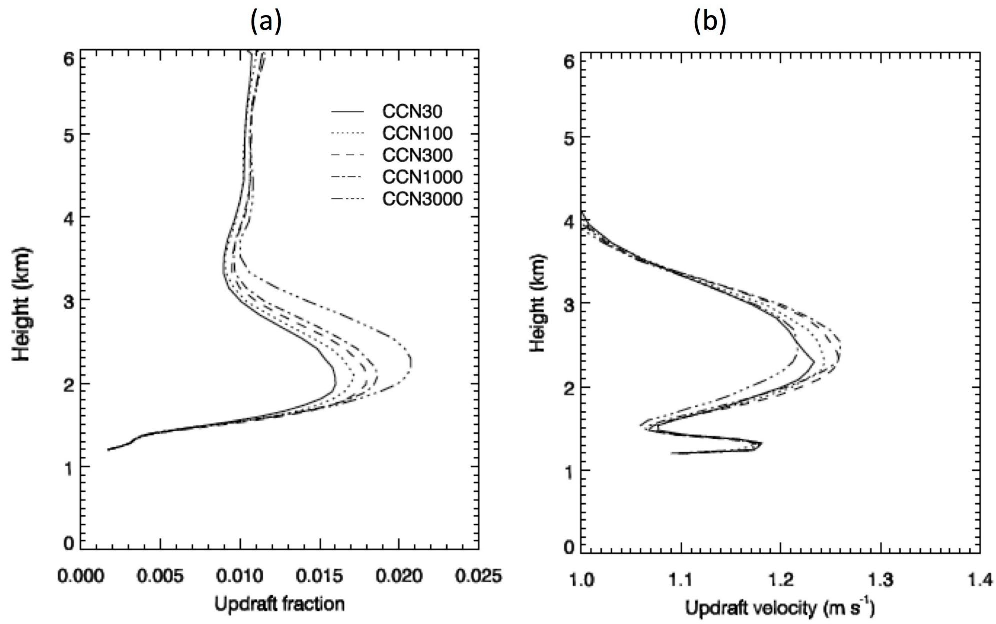

Fig. 7 (a) The fraction of updraft grid points with vertical velocity larger than 1 m s^{-1} relative to the total domain grid points, and (b) the mean updraft velocity for the grid points larger than 1 m s^{-1} over 1400-1600 UTC for the CMOC case.

Atmos. Chem. Phys. Discuss., doi:10.5194/acp-2016-772, 2016
Manuscript under review for journal Atmos. Chem. Phys.
Published: 31 August 2016

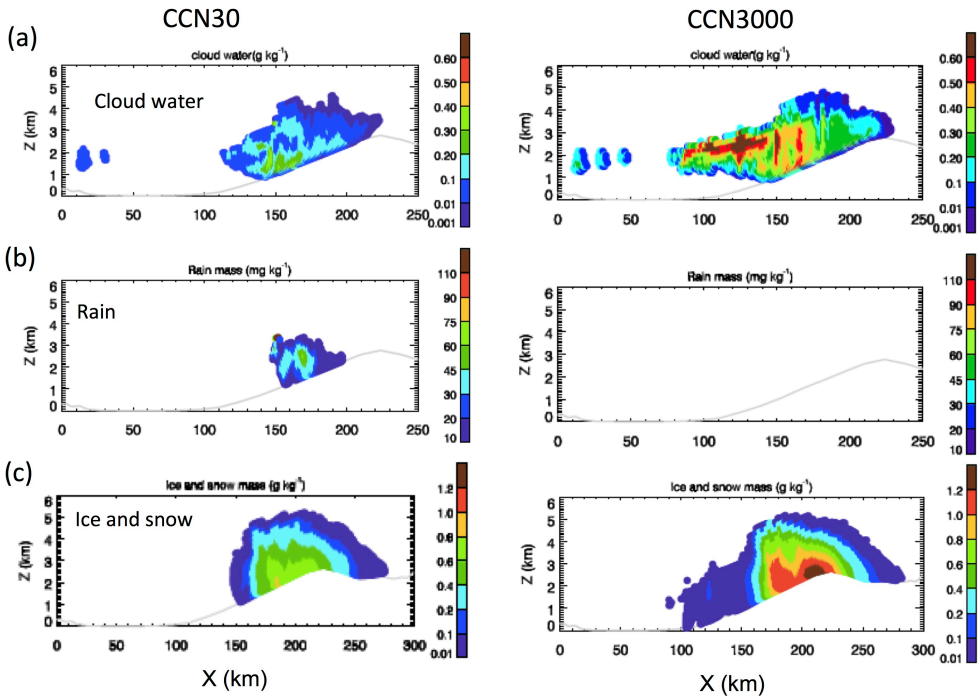

Fig. 8 The west-east cross section of (a) cloud water content, (b) rain water content, and (c) ice and snow water content for CCN30 (left) and CCN3000 (right) with INP of 1 cm^{-3} at 1400 UTC averaged over the 20 km wide area zonally for the CMOC.

Atmos. Chem. Phys. Discuss., doi:10.5194/acp-2016-772, 2016
Manuscript under review for journal Atmos. Chem. Phys.
Published: 31 August 2016

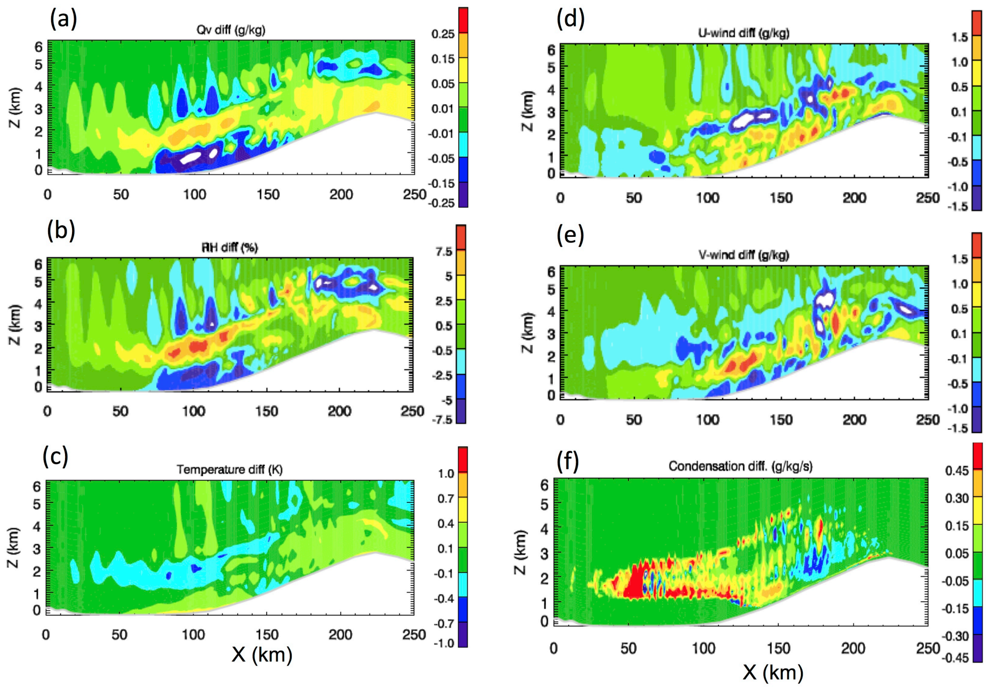

Fig. 9 Differences of (a) water vapor, (b) RH, (c) temperature, (d) U-component of the wind, (f) V- component of the wind, and (f) condensation rate between CCN3000 and CCN30 with INP of 1 cm^{-3} for the CMOC. The cross section area is same as Fig. 8. The time is at 1400 UTC except that the condensation rate used for the difference calculation is the sum of that from 1300-1400 UTC to show an accumulated value over 1-hour period before 1400 UTC.

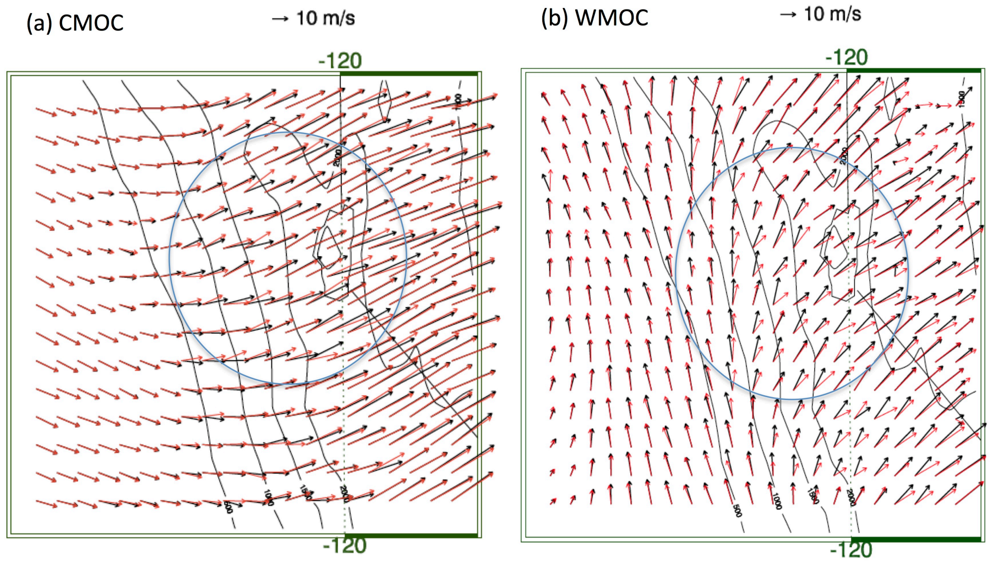

Fig. 10 The spatial distribution of wind field at about 1.7 km above the ground for (a) CMOC and (b) WMOC at 1400 UTC. The red color denotes CCN3000 and black color denotes CCN30 with INP of 1 cm^{-3}. The blue cycle is to mark the area with significant changes of wind (i.e., over the wind ward slope of the Mountain).

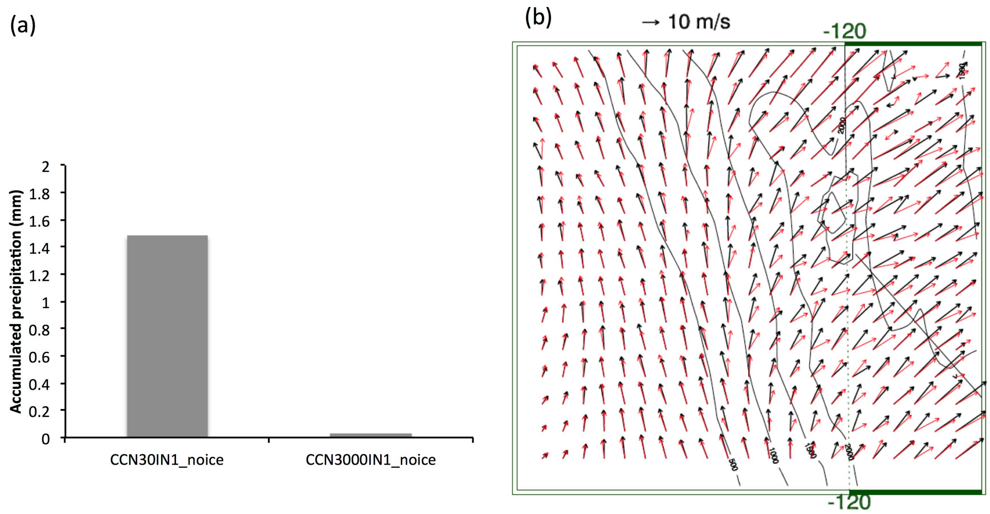

Fig. 11 Results for the two simulations without ice-related microphysics, i.e., CCN30IN1_noice and CCN3000IN1_noice, which are based on CCN30IN1 and CCN3000IN1, respectively, for the WMOC case: (a) the domain averaged accumulated precipitation, and (b) the spatial distribution of wind field at about 1.7 km above the ground at 1400 UTC. The red color on (b) denotes CCN3000IN1_noice and black color denotes CCN30IN1_noice.

Atmos. Chem. Phys. Discuss., doi:10.5194/acp-2016-772, 2016
Manuscript under review for journal Atmos. Chem. Phys.
Published: 31 August 2016

Atmospheric Chemistry and Physics Discussions

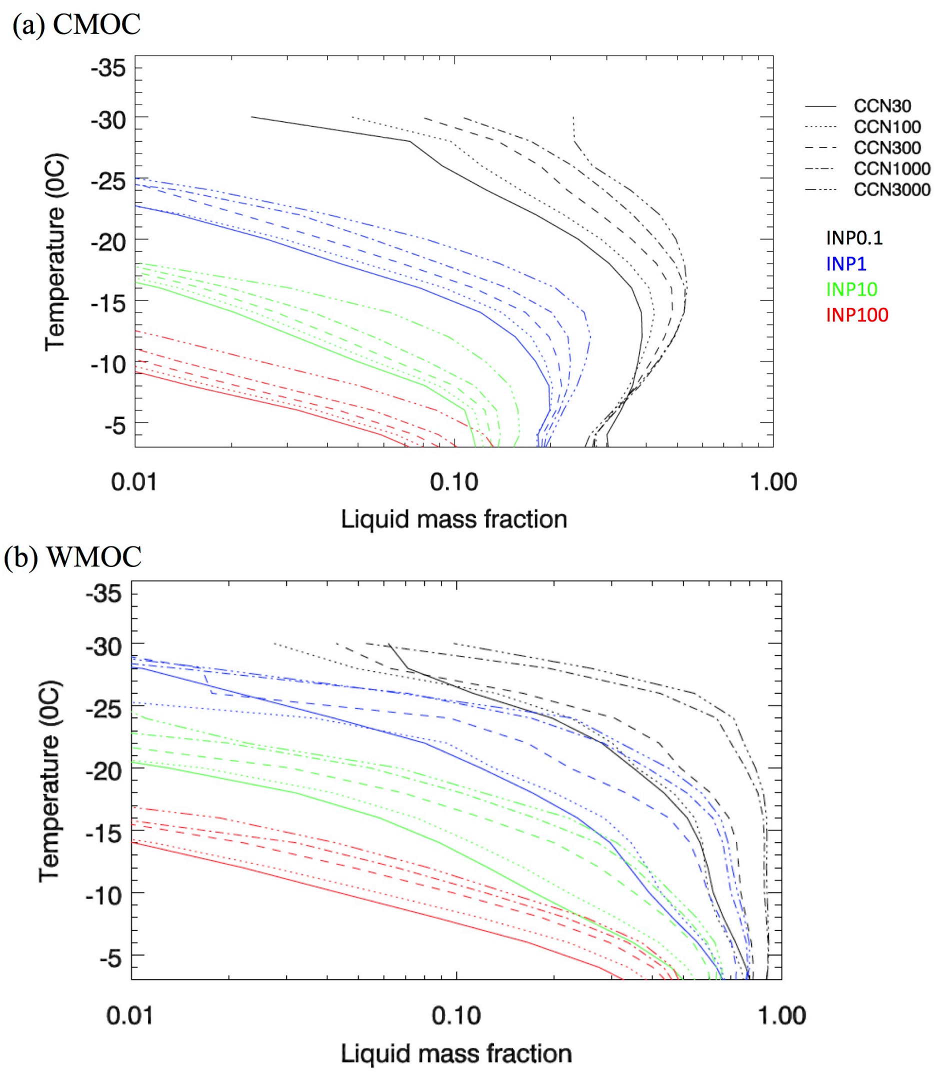

Fig. 12 The liquid mass fraction vs. temperature for the (a) CMOC and (b) WMOC over the simulation time by excluding the initial two hours. The liquid mass fraction is calculated for each temperature bin of a 2 K interval based on the total liquid water mixing ratio (droplets + raindrops) divided by the total condensate mixing ratio. The different line styles denote different CCN concentrations and different colors denote different INP concentrations.

Atmos. Chem. Phys. Discuss., doi:10.5194/acp-2016-772, 2016
Manuscript under review for journal Atmos. Chem. Phys.
Published: 31 August 2016

Atmospheric Chemistry and Physics Discussions
Open Access

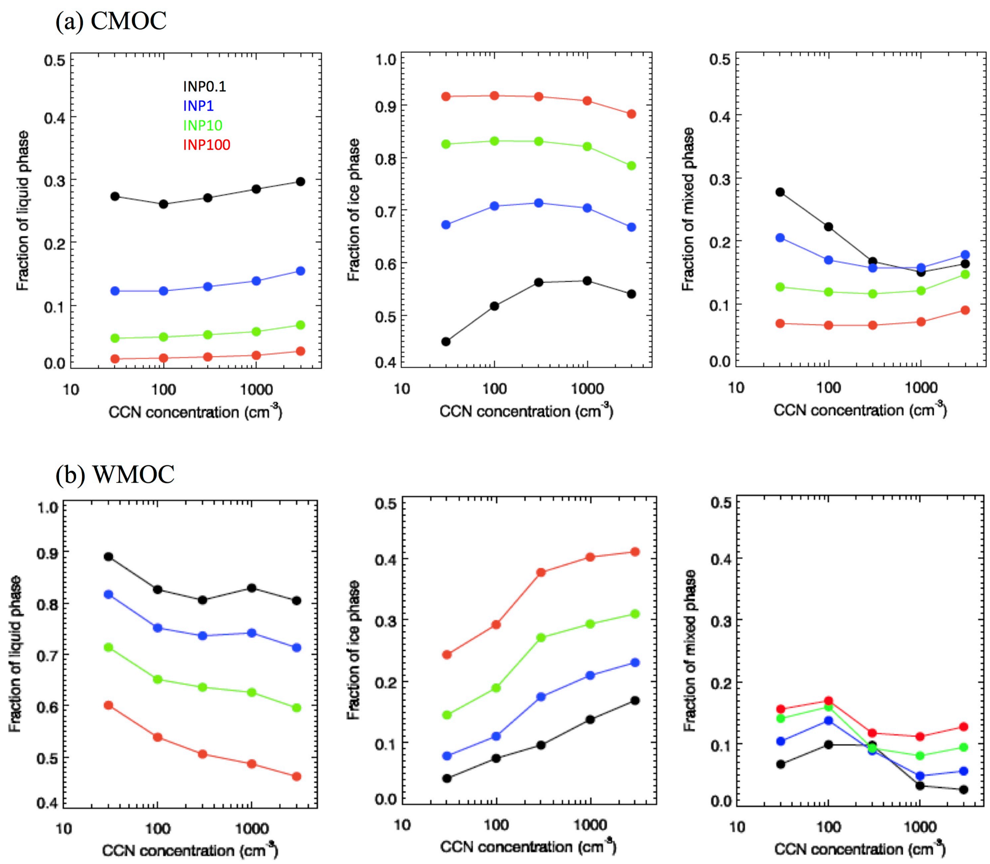

Fig. 13 The fraction of the liquid phase (left), ice phase (middle), and mixed-phase (right) for the (a) CMOC and (b) WMOC over the simulation period by excluding the initial two hours. The cloud phase for each cloud grid point that has a total condensate mass of larger than 1x10^{-5} kg kg^{-1} is identified based on the ratio of liquid to ice water mixing ratios. If the ratio is larger than 0.99 or smaller than 0.01, the grid point is identified as liquid phase or ice phase, respectively. Between these values is identified as mixed-phase. The fraction for each cloud phase is calculated by the number of grid points identified for the phase divided by the total number of the grid points of all three phases. So, the fractions of all three add up to 1 for each simulation case.

Atmos. Chem. Phys. Discuss., doi:10.5194/acp-2016-772, 2016
Manuscript under review for journal Atmos. Chem. Phys.
Published: 31 August 2016

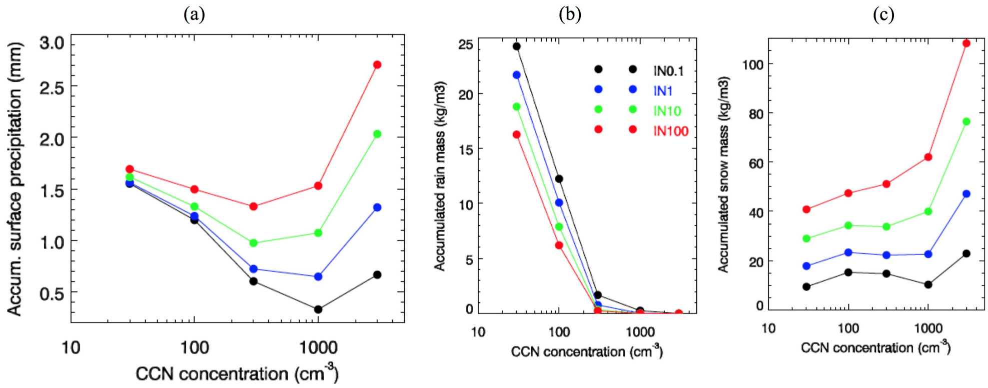

Fig. 14 Same as Fig. 2, except for the WMOC case.

Atmos. Chem. Phys. Discuss., doi:10.5194/acp-2016-772, 2016
Manuscript under review for journal Atmos. Chem. Phys.
Published: 31 August 2016

Atmospheric Chemistry and Physics
Discussions

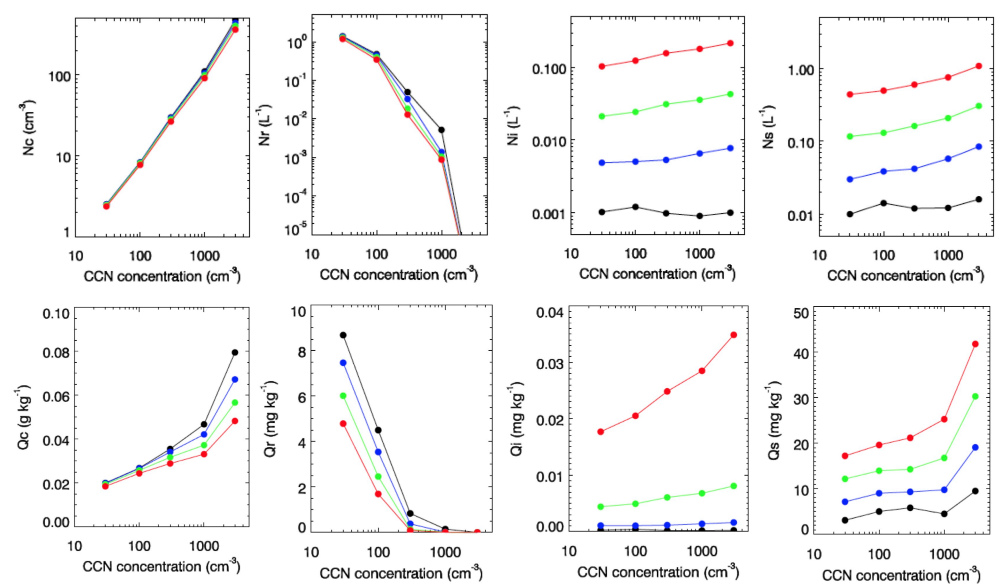

Fig. 15 Same as Fig. 3, except for the WMOC.

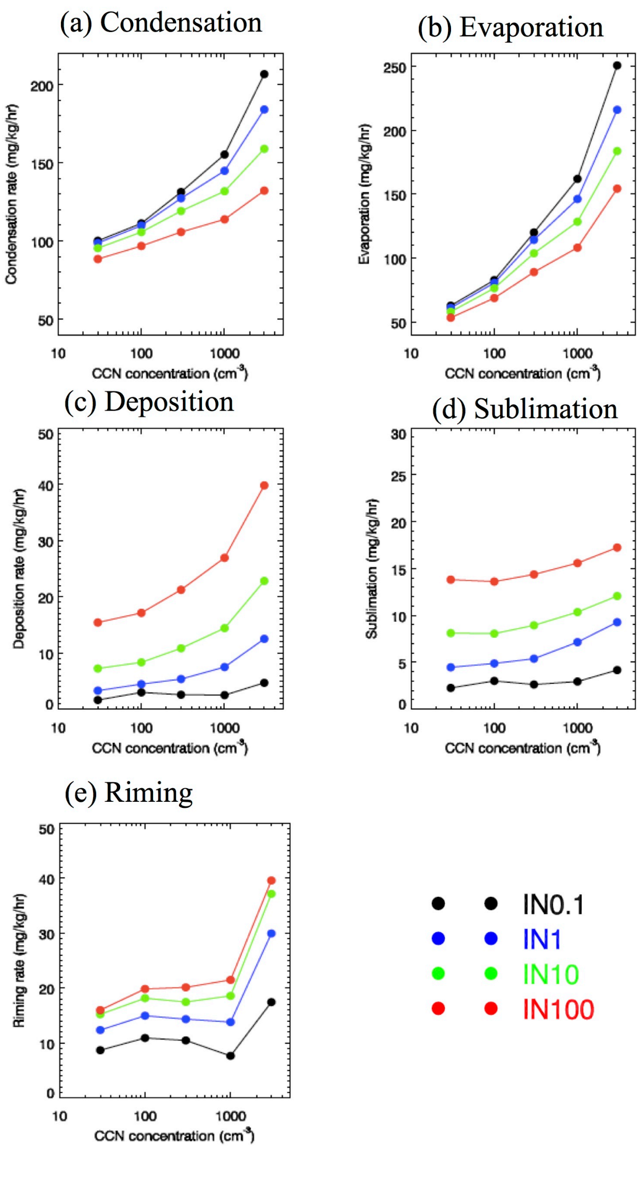

Fig. 16 Same as Fig. 4, except for the WMOC.

Atmos. Chem. Phys. Discuss., doi:10.5194/acp-2016-772, 2016
Manuscript under review for journal Atmos. Chem. Phys.
Published: 31 August 2016

Atmospheric Chemistry and Physics
Discussions
Open Access

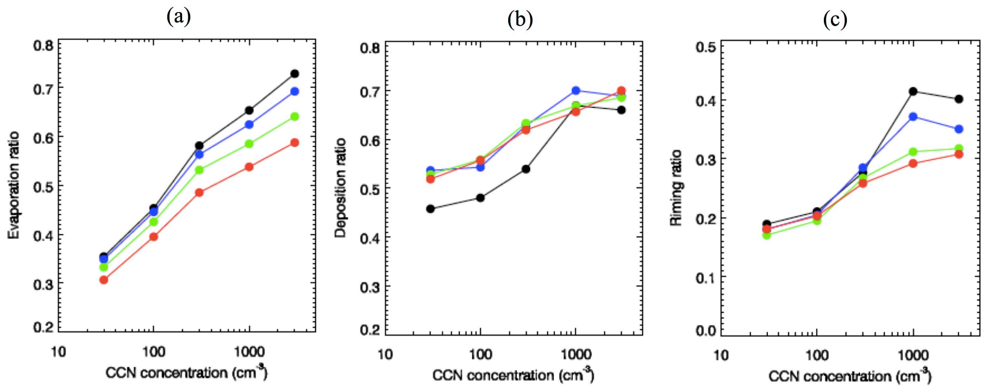

Fig. 17 Same as Fig. 5, except for the WMOC.